

Using Geophysical Methods to Image Near-Surface Cylindrical Pipeline: A Case Study on Engineering Applications, Jordan

*Hani Al Amoush*¹⁾ and *Atif Mashagbeh*²⁾

¹⁾ Lecturer, Institute of Earth and Environmental Sciences, Al al-Bayt University, Jordan
Correspondent Author, hani1@aabu.edu.jo

²⁾ Geophysicist, Institute of Earth and Environmental Sciences, Al al-Bayt University, Jordan

ABSTRACT

Conventional and modern geophysical methods have become presently very popular and reliable tools to investigate the near- surface underground features for different applications, such as engineering, geotechnical, environmental and groundwater aquifer characterization. Geophysical prospecting techniques have gained great importance due to their non-invasive, cost- effective and fast field implementation. In this research, a geomagnetic survey and an electrical resistivity survey were used to investigate the magnetic and electrical resistivity anomaly responses and imaging of an underground Gas Pipeline (GPL). This GPL is in fact part of a major multinational project to transport gas from Egypt to Jordan and then to Syria, Lebanon and Turkey. Thus it crosses Jordan from Aqaba in the south to the Jordanian-Syrian borders in the north. The two geophysical methods were successful in locating and imaging the underground GPL down to depths of 1 to 4 meters within different soil materials. The geophysical response revealed the GPL in terms of its dimensions and extension. In addition, the geoelectrical study proved to be an effective tool in mapping the subsurface lithology variations and shallow structural features such of interest (e.g. fractures, cracks and joints). Thereby, this shows the advantages of geophysical techniques in identifying the optimum site for excavation in case of any encountered trouble that could occur in a similar sub-surface engineering construction, in terms of reducing the amount of excavation to be made.

KEYWORDS: Geomagnetic, Near Surface-Geophysics (NSG), Gas Pipeline (GPL), Environmental geophysics, Resistivity, Cylindrical pipeline.

INTRODUCTION

The Near-Surface Geophysical (NSG) methods have been widely used in many environmental, engineering and geotechnical problems, e.g. for detecting underground pipes and buried infill within sink-holes, landfill investigations, sub-surface collapse features and buried foundations (McDowell, 1975; Sowerbutts, 1988; Roberts et al., 1990; Reynolds, 1998). The application of 2-D resistivity imaging methods to such geotechnical

problems and site characterization is well documented in literature (Louis et al., 2002; Dahlin, 1996). These were also recently to investigate leakage through an artificial dam body (Al Omosh et al., 2008).

In the present study, a 2-D resistivity model using Wenner configuration and geomagnetic surveys was carried out on a flat area covering an existing semi infinite-cylindrical Gas Pipeline (henceforth GPL). This GPL is forming a part of a large international project that transports gas in liquid phase from its resources in Egypt to Jordan and then to Syria, Lebanon and Turkey. Because the GPL has a cylindrical shape and extends for

thousands of kilometers, it was considered a semi-infinite cylindrical GPL in our study, and it was not working at the time of performing geophysical surveys. The surface expression and geographical extension of this GPL are well-known. However, such subsurface features don't always provide a surface expression. Therefore, the geophysical data acquired over a known subsurface GPL aimed at determining if there is a distinct anomaly that might be used to predict the locations of subsurface causative features in other geophysical applications, since the present underground GPL is an air-filled pipe with predefined dimensions, and hence exhibits high geophysical contrast and behaves like different subsurface geological features such as subsurface cavities. Another objective of this paper is to study the effect of this underground pipeline on local earth's magnetic field and also on the earth material resistivity heterogeneities.

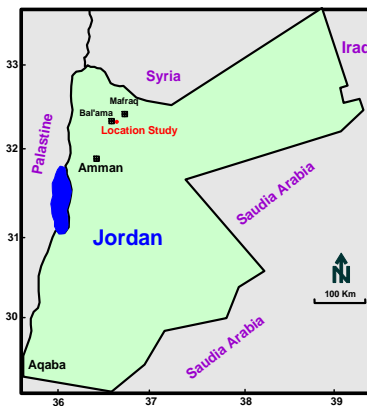


Figure (1): Location map of the study area.

Site Description and Geological Setting

The area of the study is located to the south-east of Bal'ama region at about 35 km south-west of Mafraq city (Fig. 1), with coordinates [N 32° 14' 01.95", E 36° 06' 43.27"]. The study area is almost flat with an altitude of 639 amsl (Fig. 2). It was necessary for the experiment site and measuring stations to be apart from any suspected causative magnetic or electrical noises such as electric power lines, water pipeline supply, cultural features or any other possible geophysical noise. Thick accumulation

of soil materials is covering the area of study, south-dipping layers of limestone and silicified limestone of Wadi Al-Sir formation (A7) are outcropping around the area (Abed, 2000). GPL is extending from south to north and is lying beneath the ground surface by about two to three meters, within the soil accumulation zone. The conceptual model of the GPL beneath earth's surface and the lines of geophysical surveys are illustrated in a 3-D block diagram (Fig .3).

METHOD AND INSTRUMENTATION

Geomagnetic Study

In the present study, a high resolution geomagnetic survey was applied along a set of profiles on the ground surface over an existing near-surface GPL. The spacing between each measuring station and the other was 1 m. These measurements are eventually forming a grid. As mentioned before, the GPL is considered as a cylindrical pipe, having about (36 inch = 92 cm) diameter and lying beneath the ground surface down to about 1.5-3 meters. The orientations of the geomagnetic profiles were laid out to be perpendicular to the target strike (Figs.3 and 4).

A proton precession magnetometer instrument (Geometrics type-820) was used for gathering the field measurements. This device measures the total magnetic field intensity with an accuracy of about 0.1 nanoTesla (nT) (Dobrin and Savit, 1988). A base station to record the total magnetic field was chosen near the study area, aiming at monitoring the time variations in the earth's magnetic field caused by magnetic storms and diurnal variations (Fig. 5). However, no significant variations in the total magnetic intensity have been measured at the base station during the field survey. Post-processing techniques allow for the removal of time variations in the datasets within the grid, thus the anomalies produced in the post processed datasets are presumably caused by subsurface materials (Breiner, 1999), the elevation corrections are normally not required in ground magnetic surveys (Sharma, 1997). The residual magnetic anomaly caused by the subsurface GPL was estimated based on the removal of the regional magnetic field due to the deep

magnetic sources from the measured magnetic intensity values, and this was actually done by assuming a zero-level and the corrected magnetic intensities were adjusted for the zero-level by adding or subtracting the measured data to produce the residual anomaly. The selected zero-level was estimated based on the measurements of

magnetic intensities at the base station and also from the IGRF published map. Figures (6, 8, 10, 12 and 14) show the variations of the corrected total magnetic field intensity along different profiles. Residual magnetic anomaly for each profile is presented in Figures (7, 9, 11, 13 and 15).

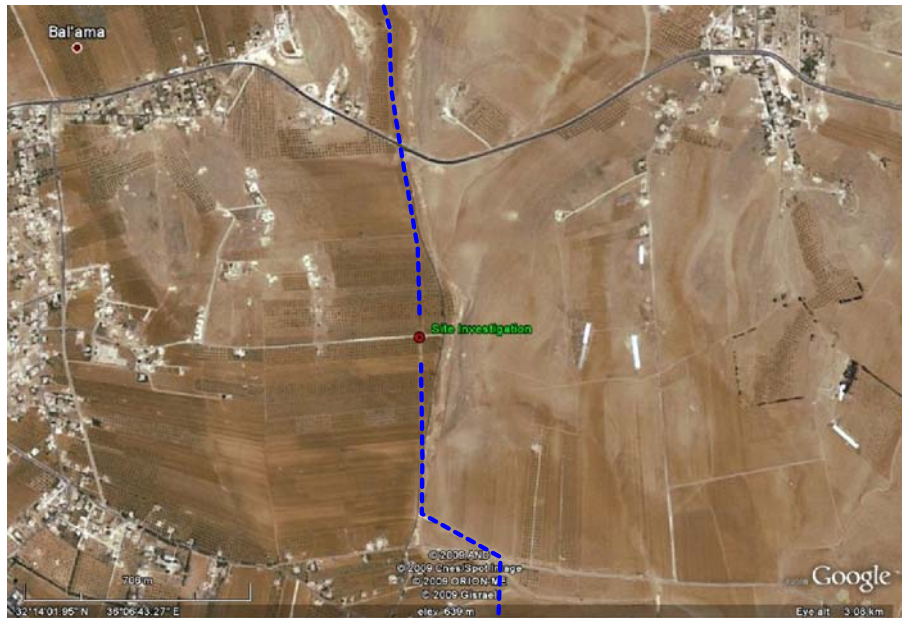


Figure (2): Location of the experiment site showing a part of GPL extension.

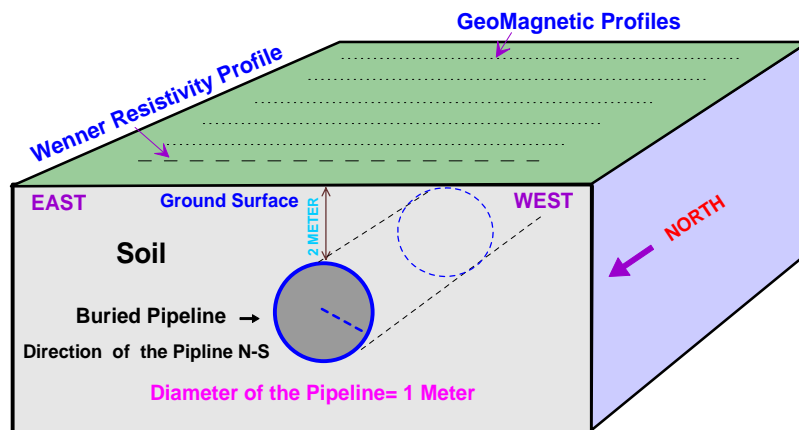


Figure (3): A 3-D block diagram illustrating the extension of GPL beneath ground surface and surface geophysical survey lines.

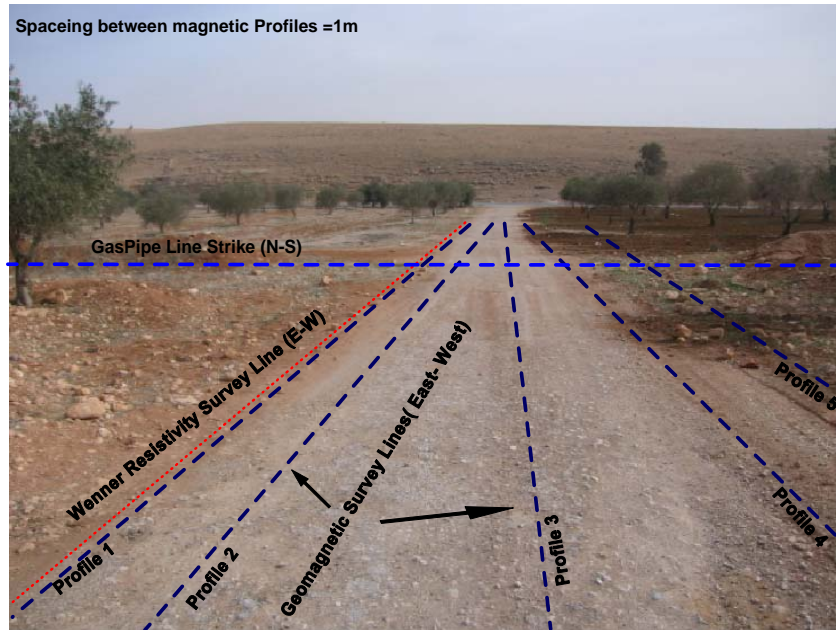


Figure (4): Extensions of geophysical profiles with respect to the GPL strike.

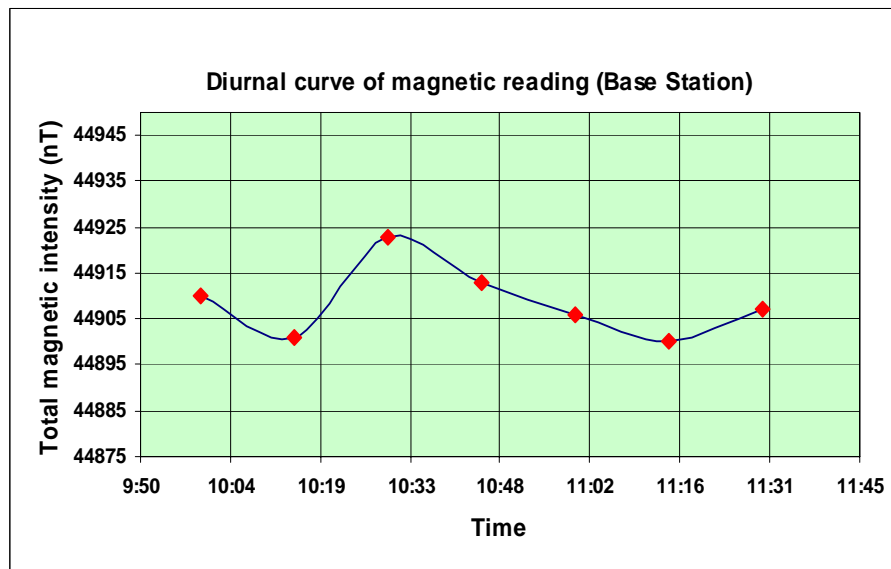


Figure (5): Diurnal variations curve of magnetic reading.

Electrical Resistivity Study

Resistivity surveys measure variations in electrical resistivity of the ground through applying a small electric current across arrays of electrodes; it involves the passage

of direct current into the ground via electrodes and the measurement of the potential difference between some sections of the subsurface (Telford et al., 1990). In our surveys, an ABEM campus Geopulse Resistivimeter -

Birmingham, England instrument was used for data collection. It is a digital signal enhancement device incorporating a microprocessor that gives the resistance (R) reading in Ω , $m\Omega$ or $\mu\Omega$ and is capable of accurate measurements over a wide range of conditions. The collected data were converted into resistivity readings that can be then modeled in order to provide information about the lateral and vertical variations of resistivity of the subsurface materials. The apparent resistivity was found by the equation:

$$\rho_a = 2\pi aR \quad (1)$$

Where (ρ_a) is the apparent resistivity measured in (ohm.m), a is the electrode separation (m) and R is the resistance as measured in the field (ohm) (Telford et al., 1990).

In the present study, a Wenner configuration of resistivity profiling method was applied in order to provide information about the lateral variations of resistivity of the subsurface which imply to our target (the GPL), since this configuration is very sensitive to the lateral inhomogeneities, the electrode spacing is kept fixed and the entire array is moved along a profile, while the apparent resistivity is recorded at discrete intervals along the profile (Reynolds, 1998). The survey was conducted along a line perpendicular to the extension of the GPL strike (Figs.3 and 4); the length of the resistivity survey line is 40 meters. Resistivity survey lines at seven electrode separations (a) were carried out and these are ($a = 1$ m, $a = 2$ m, $a = 3$ m, $a = 4$ m, $a = 5$ m, $a = 6$ m and $a = 7$ m). The center point of the profile between potential electrodes was defined as the point of measurement (Griffiths et al., 1985).

RESULTS AND DISCUSSION

Geomagnetic Survey Results

The corrected magnetic measurements would be more expressive if they were presented in the form of profiles or contour maps. From these, it would be possible to conclude, even through qualitative interpretation, the site and boundaries of highs and lows in magnetic anomalies relating the target GPL. In the following part, this interpretation is applied for the five total magnetic field

intensity profiles and the resulting anomaly across the study area.

Geomagnetic Profile 1

This profile extends from the east to the west direction along 21 meters (Fig. 6), crossing the location of GPL at a possible distance within $x = 10$ m to $x = 14$ m. Figure (6) shows a slight gradual increase in the total magnetic field intensity from a distance $x = 1$ m to $x = 10$ m, then it decreases abruptly by about (8000 nT), just within a horizontal distance of $x = 2$ meters. From $x = 15$ m to the end of the profile, it shows a slight decrease in the total magnetic intensity. The resulting magnetic anomaly (Fig. 7) reveals the presence of two small positive anomalies (peak) and one large negative anomaly (trough); the shape of the anomaly is produced according to local disturbance in the earth's magnetic field due to the buried magnetic object (GPL) which is a function of many factors (i.e., the declination of the magnetic field, the trend of the buried GPL (N-S), the trend of the survey line (E-W) and the inclination angle of the earth's magnetic field).

Geomagnetic Profile 2

It extends about 21 m in a westerly direction; it is parallel to profile 1. Figure (8) shows the variations of the total magnetic field intensity along this profile; however, it exhibits an almost different behavior of the total magnetic intensity of profile 1. The total magnetic intensity increases gradually to a distance $x = 9$ m, and becomes larger than 46000 nT, after that, it abruptly decreases to 44500 nT, just within a horizontal distance of 3 meters. From a distance $x = 12$ m to the end of the profile, it represents a stability in the magnetic intensity. The resulting magnetic anomaly (Fig. 9) reveals the presence of one positive anomaly (from $x = 3$ m to $x = 11$ m), and another negative magnetic anomaly from $x = 11$ m to the end of the profile. The negative anomaly is well correlated with the presence of subsurface GPL, as it is compared with the previous profile. The positive anomaly may result from the magnetizing source in the subsurface and might be the body of the GPL.

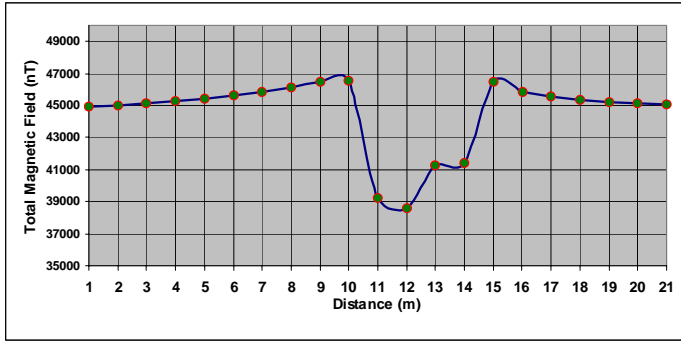


Figure (6): Total magnetic field along profile 1.

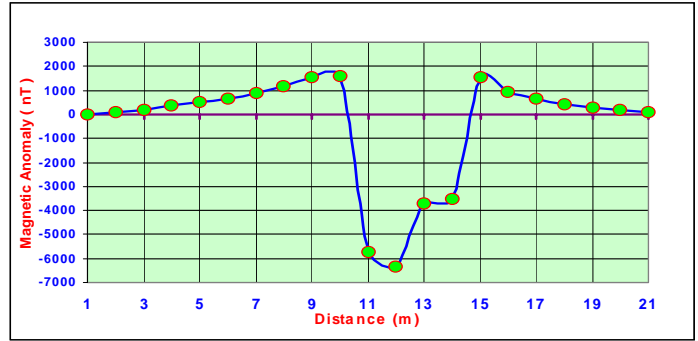


Figure (7): Magnetic anomaly along profile 1.

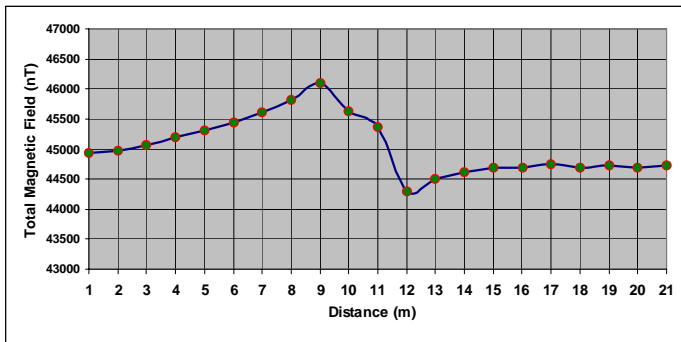


Figure (8): Total magnetic field along profile 2.

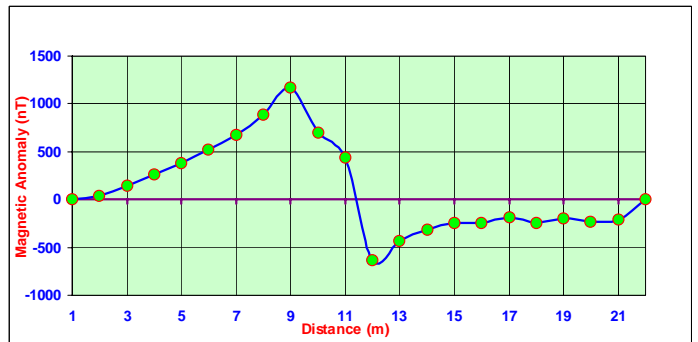


Figure (9): Magnetic anomaly along profile 2.

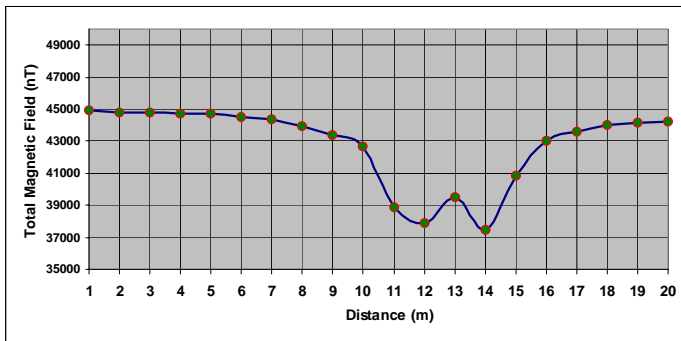


Figure (10): Total magnetic field along profile 3.

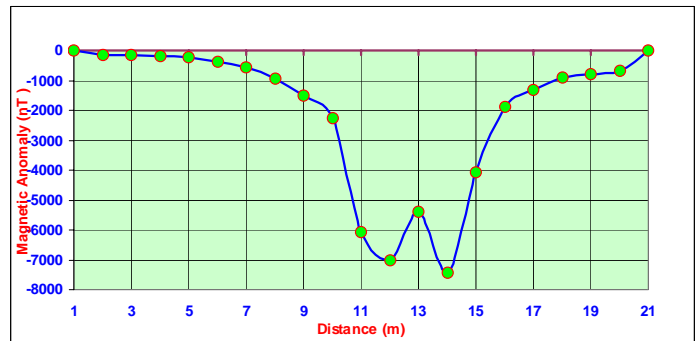


Figure (11): Magnetic anomaly along profile 3.

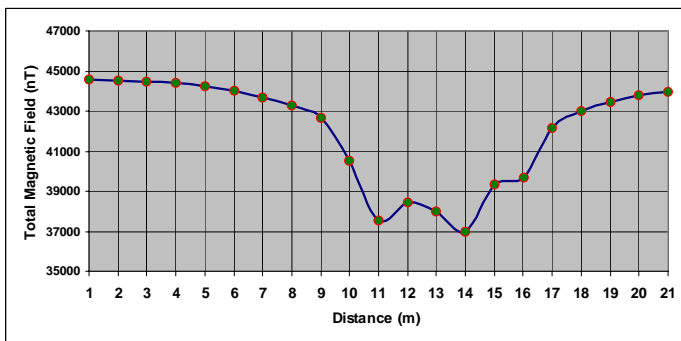


Figure (12): Total magnetic field along profile 4.

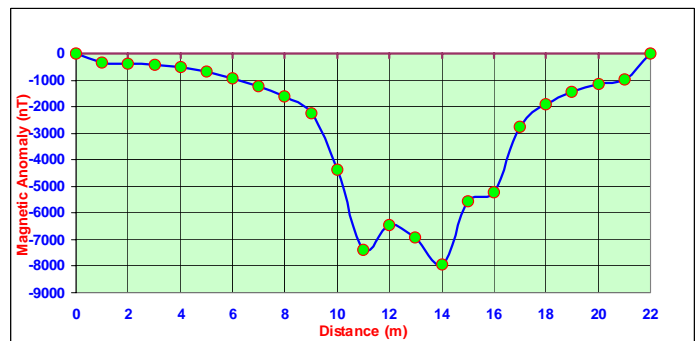


Figure (13): Magnetic anomaly along profile 4.

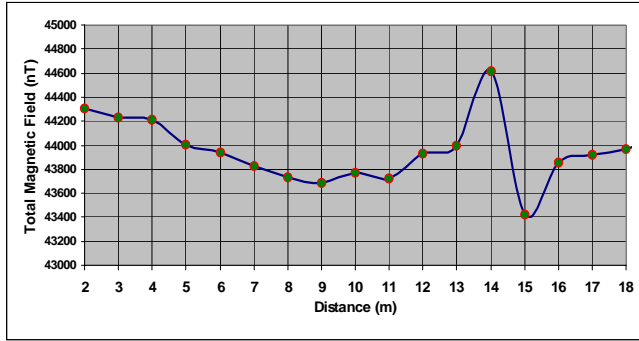


Figure (14): Total magnetic field along profile 5.

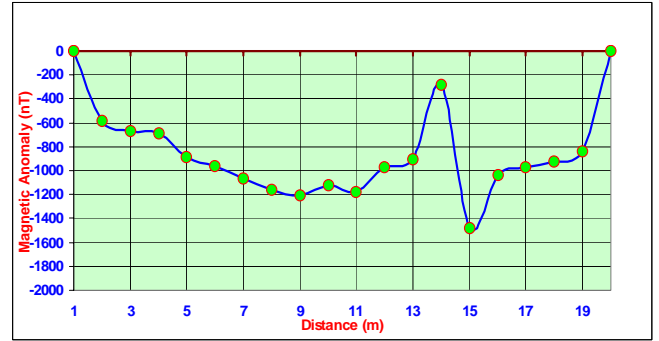


Figure (15): Magnetic anomaly along profile 5.

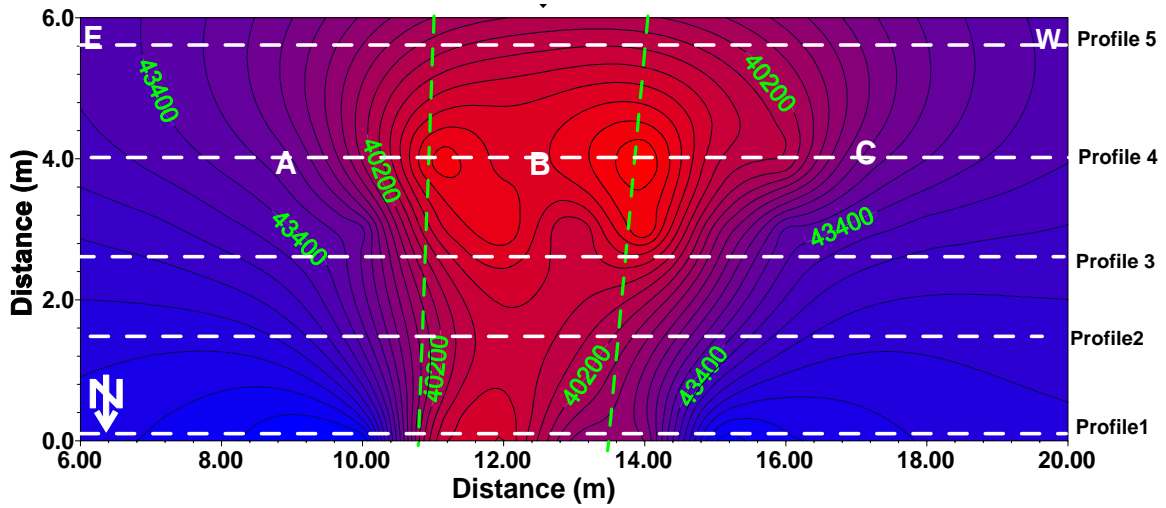


Figure (16): Contour map of total magnetic field over the buried GPL (The white dashed line indicates the trace of east-west geomagnetic profiles).

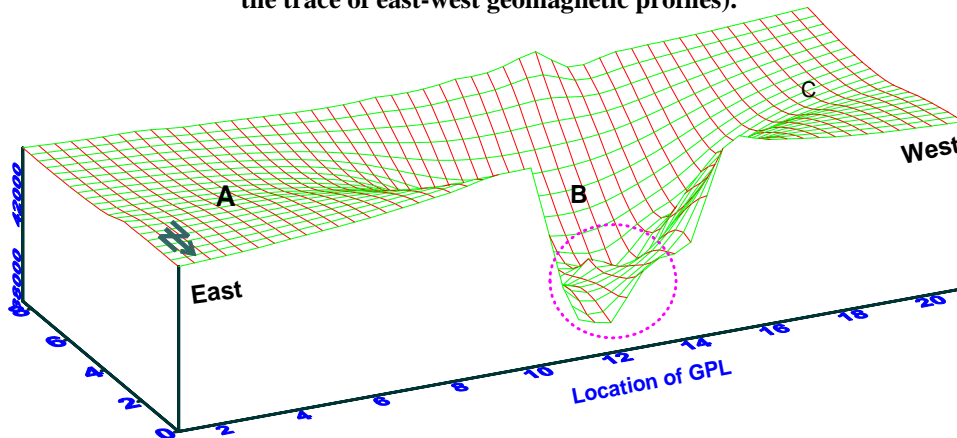


Figure (17): 3-D block diagram illustrating the second derivative of the total magnetic field and the main magnetic anomalies (B).

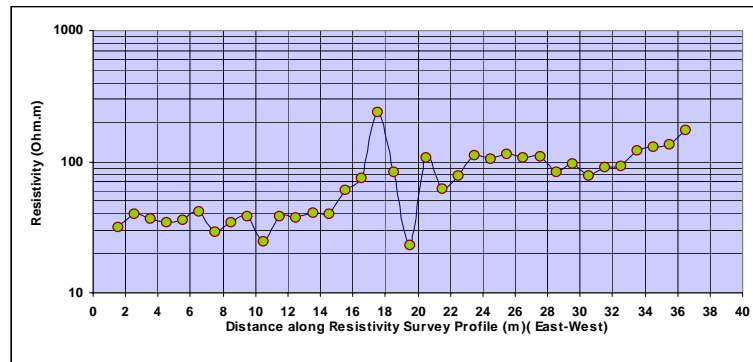


Figure (18): Electrical resistivity variations at electrode separation ($a = 1$ m).

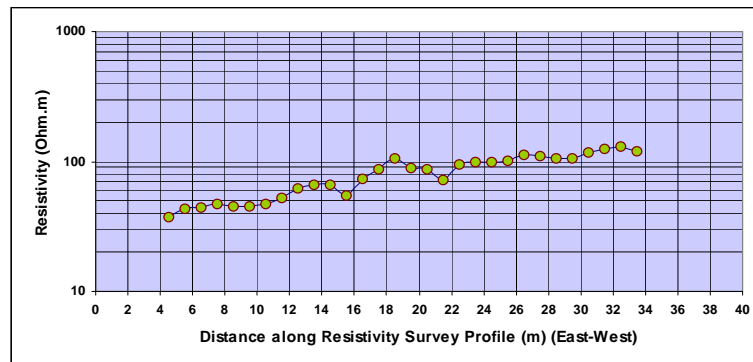


Figure (19): Electrical resistivity variations at electrode separation ($a = 3$ m).

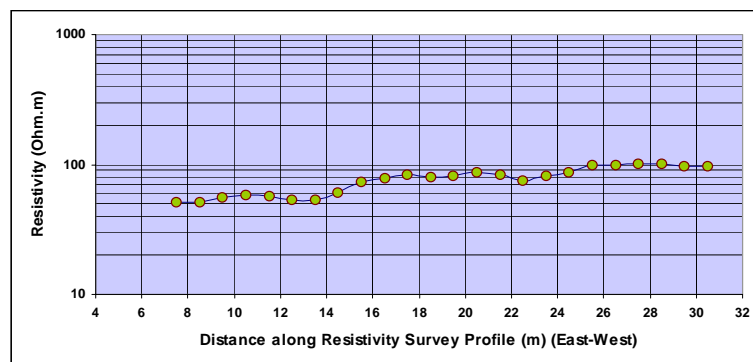


Figure (20): Electrical resistivity variations at electrode separation ($a = 5$ m).

Geomagnetic Profile 3

It extends about 20 m from east to west direction. The total magnetic intensity curve in (Fig. 10) shows a stability in the magnetic intensity from the distance $x = 1$ m to $x = 6$ m, and then the magnetic intensity begins to be affected by the underground pipeline, and it slightly decreases gradually to a distance $x = 9$ m, after that, a large decline in the magnetic intensity by about 4500 nT - just within a horizontal distance of 3 meters- is clearly shown. From a distance $x = 14$ m to $x = 16$ m, an abrupt increase in the magnetic intensity is shown, and then the curve starts to be more stable and the effect of the underground pipeline is eliminated to the end of profile. The resulting magnetic anomaly in (Fig. 11) reveals the presence a one large negative trough anomaly with an amplitude reaching more than 7000 nT, this negative anomaly is interpreted by the effect of the air-filled pipeline which produces a very low magnetic susceptibility (k) since it is a vacuum pipe line where $k = 0$.

Geomagnetic Profile 4

Figure (12) shows the variations of total magnetic fields along this profile, and the resulting magnetic anomaly is presented in Fig (13). To a great extent, the magnetic interpretation of these curves is similar to the interpretation of profile 3, which supports and reveals the presence of a large negative trough anomaly with an amplitude reaching 7000 nT, produced by the very low magnetic susceptibility air-filled underground pipeline.

Geomagnetic Profile 5

It extends about 18 m in a westerly direction. Figure (14) shows the total magnetic field variations. The resulting magnetic anomaly curves are presented in (Fig. 15). They exhibit a large negative trough anomaly including a magnetizing noise indicating the effect of the underground pipeline in the subsurface.

Geomagnetic Contour Map

In order to prepare a geomagnetic contour map, it was necessary to reduce the field data in a regular grid by interpolation. In this study, a surface mapping system (Surfer Version 8.0, 2002) software was used to grid and

interpolate the magnetic field intensity measurements and display results as a geomagnetic contour map as shown in (Fig. 16). It is obvious from Fig. (16) that the major magnetic anomaly is the negative anomaly (zone B) which is indicating to the underground GPL. The second derivative is a mathematical technique used in potential field data enhancement and interpretation; it amplifies the short-wavelength information at the expense of the long-wavelength information, so it is sometimes used to locate the edges of magnetic bodies and to emphasize the sources at shallow depths (Dobrin and Savit, 1988). In this study, the second derivative of the total magnetic field was calculated using the mentioned software to clarify the shallow magnetic anomalies. These were displayed as a three-dimensional block diagram in (Fig. 17).

Geo-electrical Survey Results

Wenner Arrays

Measurements of electrical resistivity were carried out using conventional Wenner configuration aiming to obtain sufficient information about the lateral variations of the shallow subsurface features and give a clear image about the presence of the underground GPL. In Wenner array, each potential electrode is separated from the adjacent current electrode by a distance (a) called electrode separation or spacing which is one-third the separation of the current electrodes (Dobrin and Savit, 1988). In the following part are interpretations of the geo-electrical profiles at selected electrode separations.

Resistivity at Electrode Separation $a = 1$ meter

Figure (18) shows the electrical resistivity variations along the survey line; it extends from the east to the west direction (Fig. 4) and shows a general increasing trend. Two prominent subsurface rock types can be recognized: one with an average apparent resistivity of 40 ohm.m represented by the right segment of resistivity curve between $x = 1$ m and $x = 15$ m which may reflect a high thickness of soil materials, and the other with an average resistivity of 100 ohm.m represented by the left segment of the resistivity curve between $x = 21$ m and $x = 36$ m, which may indicate a mixture of soil and rock debris

materials (western part of the study area). The resistivity curve also reveals the presence of a significant zone with anomalously high resistivity followed by low resistivity within the distances $x = 17$ m to $x = 20$ m (Fig. 18). This electrical anomaly is highly correlated with the presence of the subsurface GPL which acts as a vertical boundary. The large undulation in the resistivity curve that arises above the GPL and takes a W-shape is due to the

positioning of the electrodes relative to the vertical boundary represented by the GPL, since the W-shape in resistivity curve is a characteristic for Wenner configuration in regions having vertical boundary (Telford et al., 1990), while the small undulations that arise in the remaining resistivity curve could be ascribed to the presence of cracks, fissures and joints within the shallower subsurface materials.

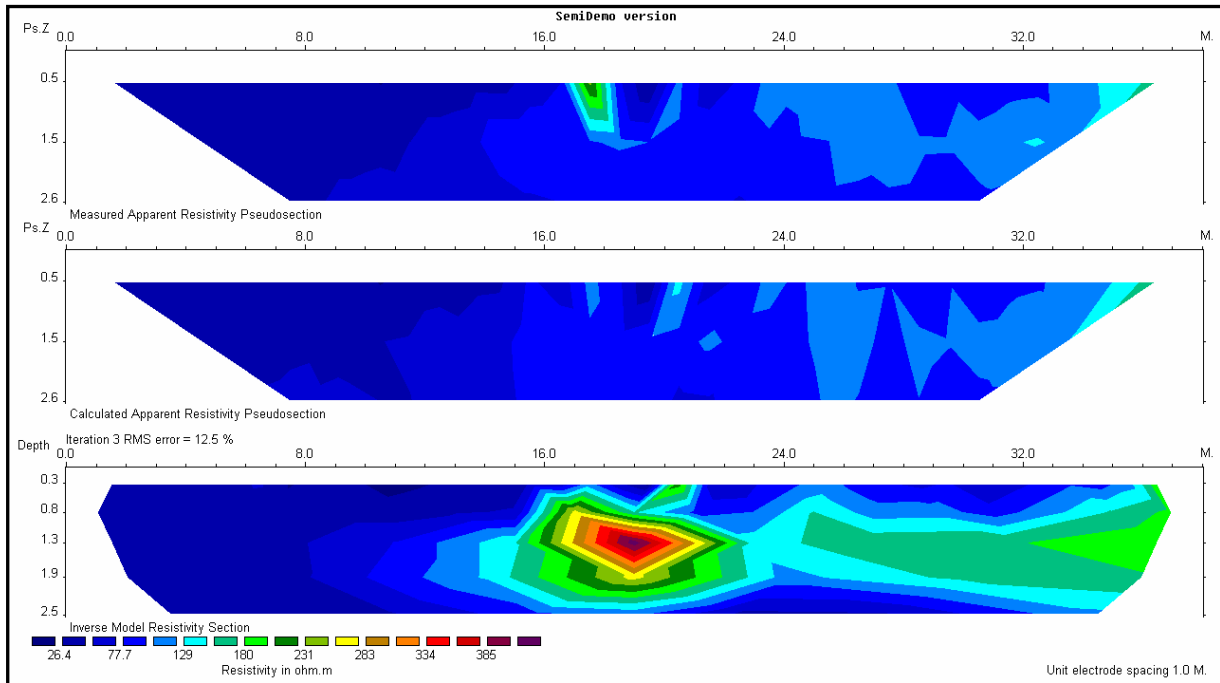


Figure (21): 2-D resistivity section across the GPL strike line.

Resistivity at Electrode Separation $a = 3$ m

The resistivity variations along the survey line at electrode separation $a = 3$ m are presented in (Fig. 19), which exhibits a general increase in resistivity in westerly direction. As in the previous electrode separation ($a = 1$ m), the two prominent subsurface rock types can be recognized. The response of the underground GPL for electrical resistivity at this separation is clearly shown in the resistivity curve as a W-shape at distances $x = 14$ m- $x = 16$ m- $x = 18$ m- $x = 21$ m- $x = 22$ m, with a maximum peak at the distance $x = 18$ m (Fig. 19).

Resistivity at Electrode Separation $a = 5$ m

The resistivity variations at electrode separation $a = 5$ m is presented in (Fig. 20). The general westerly trend of increasing resistivity is still being seen. There are no other significant features that can be drawn from this resistivity curve. The effect of the underground GPL almost disappears in resistivity curves at this electrode separation.

Resistivity Data Processing

Although the apparent resistivity measurements were

collected using the conventional Wenner configuration method, it was possible to transform the field dataset into a format that can be readable by the software RES2DINV for data processing and modeling. RES2DINV is a program that automatically generates a two-dimensional resistivity model for subsurface from field data measurements (Loke et al., 1996; Loke, 1997; Loke, 1999). The inversion routine used by the program is based on the smoothness-constrained least-squares method (DeGroot-Hedlin and Constable, 1990; Sasaki, 1992). The 2-D model used by this program divides the subsurface into a number of rectangular blocks. The purpose of this program is to determine the resistivities of the rectangular blocks that will produce an apparent resistivity pseudosection which agrees with the actual measurements. The optimization method basically tries to reduce the differences between the calculated and measured apparent resistivity values by adjusting the resistivity of the model blocks. A measure of such differences is given by the Root-Mean-Squared (RMS) error. However, the model with the lowest possible RMS error can sometimes show large and unrealistic variations in the model resistivity values and might not always be the "best" model from a geological perspective. In general, the most prudent approach is to choose the model at the iteration after which the RMS error does not significantly change. This usually occurs between the 3rd and 5th iterations (Loke et al., 1996).

Geo-electrical Cross-Section Interpretation

The field measured resistivity dataset was processed and inverted using RES2DINV program and presented as a 2-D pseudo- apparent resistivity and a 2-D inverse model resistivity section (Fig. 21). It is obvious that the subsurface is characterized by the presence of two main rock types on the basis of the resistivity variations; these are: a zone of low resistivity between (35-75 ohm.m extending from $x = 1$ m to $x = 15$ m) interpreted as a thick accumulation of soil and a zone of high resistivity (>200 ohm.m extending from $x = 24$ m to $x = 35$ m) interpreted as a zone consisting of gravel and limestone boulders, chert mixed with soil materials. The underground GPL is

clearly imaged in the 2-D resistivity cross-section. Its effect appears between $x = 16$ m and $x = 21$ m on the inverted resistivity cross-section (Fig. 21), with modeled true resistivity (>250 ohm.m), its upper boundary appears at a depth of about 1m and its lower boundary appears at a depth of about 2m below ground surface, this correlates nearly well with its actual vertical depth (Fig. 4), while the horizontal extension of the anomaly appears to be wider than the real width of GPL, this is due to the digging processes and the surrounded filling materials during GPL construction. In general, the inversions gave relatively high-resolution images and revealed the geometries of the resistivity anomalous relating the subsurface GPL.

CONCLUSIONS

Geo-electrical resistivity surveys using Wenner configuration as well as a high resolution magnetic survey were applied to investigate and image a subsurface cylindrical Gas Pipeline (GPL) as a case study. The geomagnetic study reveals the presence of a clear negative anomaly that correlates with the presence of underground air-filled GPL. It provides a nearly precise delineation for its geometry through the different magnetic anomalies across profiles, magnetic field contour map and also the second derivative magnetic field intensity as a three-dimensional block diagram. Other magnetizing sources and the magnetizing response of the underground GPL body were delineated at some segments of magnetic curves.

The surface geo-electrical method used in this study was the profiling method with a Wenner configuration. The lateral variations of apparent resistivity across the GPL strike at different electrode separations were very important in the qualitative interpretation phase. The effect of GPL was very obvious at small electrode separations and it had a small effect at large electrode separations. The large W-shape variations on the apparent resistivity variations curve along the profile indicated a vertical boundary in the subsurface represented by the GPL, the small W-undulations appearing on the apparent

resistivity curves might indicate the presence of fractures, fissures and joints in the subsurface sediments. The quantitative interpretations of resistivity data aim at producing a 2-D resistivity cross-section model for the subsurface, this has been done by transforming the field dataset into a readable data format with RES2DINV program, the resulting 2-D resistivity model was successful in clarifying and imaging the underground GPL in terms of its geometry, depths and dimensions. The 2-D resistivity cross-section also shows two different subsurface rock types, thick accumulations of soil in the eastern part of the cross-section and a mixture of sediments consisting of gravel and boulders of limestone and chert at the western part of the cross-section, and this could be ascribed either to sediment-logical facies variations or shallow structural effects. Here, it is worthy to say that these lithological variations were not magnetically resolved or even shown.

REFERENCES

- Abed, A. 2000. Geology of Jordan, Publications of Jordanian Geologists Association, Amman, Jordan.
- Al-Omsh, H., Al-Farajat, M. and Zunic, F. 2008. Leakage in Bayer Dam in Jordan: Its causes and consequences. *Jordan Journal of Civil Engineering*, 2 (4): 363-375.
- Breiner, S. 1999. Application manual for portable magnetometers: San Jose, California, Geometrics, accessed April 2004 at URL <http://www.geometrics.com/>.
- Dahlin, T. 1996. 2D resistivity surveying for environmental and engineering applications. *First Break*, 14 (7): 275-283.
- DeGroot-Hedlin, C. and Constable, S. 1990. Occam's inversion to generate smooth, two-dimensional models from magneto-telluric data. *Geophysics*, 55: 1613-1624.
- Dobrin, M. P. and Savit, H. 1988. Introduction to geophysical prospecting. 4th edition, McGraw-Hall, Inc., USA, 867p.
- Golden Software .2002. Surfer 8.0, Surface Mapping Software. www.goldensoftware.com.
- Griffiths, D.J. and J. Tumbull. 1985. A multi-electrode array for resistivity surveying. *First Break*, 3:16-20.
- Loke, M.H. 1997. Electrical imaging surveys for environmental and engineering studies. A practical guide to 2-D and 3-D surveys, Penang. Malaysia, 57p.
- Loke, M. H. and Baker, R.D. 1996. Rapid least square inversion of apparent resistivity Pseudosection by a quasi-Newton method. *Geophysical Prospecting*, 44: 131-152.
- Loke, M. H. 1999. RES2DINV- rapid 2-D resistivity and IP inversion using the least squares methods. Software manual, 81p.
- Louis, I.F., Karastathis, C.V., Vafidis, P.A. and Louis, F.I. 2002. Resistivity modeling and imaging methods for mapping near-surface features: Application to a site characterization at the Ancient Temple of Olympian Zeus in Athens. *Journal of the Balkan Geophysical Society* (In Press).
- McDowell, P.W. 1975. Detection of clay filled sink-holes in the chalk by geophysical methods. *Quarterly Journal of Engineering Geology*, 8:303-310.

Acknowledgement

The authors acknowledge Dr. Adnan Al-Harabsheh, Dean of the Earth and Environmental Institute at Al-Bayt University for his cooperation and support during various phases of this research. We are indebted to Mr. Adnan Rizg for his help during the long field work, and we also wish to thank Prof. Najeeb Abou Karaki from the University of Jordan for his insightful review of this manuscript.

- Reynolds, John M. 1998. An introduction to applied and environmental geophysics, 796; Bffins Lane, Chichester, England, John Wiely and Sons, Ltd.
- Roberts, R.L., Hinz, W.J. and Leap, D.I. 1990. Data enhancement procedures on magnetic data from landfill investigations. In: Ward, S.H(ed.), *Geotechnical and Environmental Geophysics*, Vol.11: Environmental and Groundwater Tulsa: Society of Exploration Geophysicists, 261-266.
- Sasaki, Y. 1992. Resolution of resistivity tomography inferred from numerical simulation. *Geophysical Prospecting*, 40: 453-464.
- Sharma, P.V. 1997. Environmental and engineering geophysics. 1st edition, Cambridge University Press, Cambridge, 475p.
- Sowerbutts, W.T.C. 1988. The use of geophysical methods to locate joints in underground metal pipelines. *Quarterly Journal of Engineering Geology*, 21:273-281.
- Telford, W.M., Geldart, L.P. and Sheriff, R.E. 1990. Applied geophysics, 2nd edition, Cambridge University Press, Cambridge, 792p.